

Axial Burnup Effect on the Multiple Misloading Analysis for Burnup Credit Cask Design

Saed Alrawash *, Muth Boravy, Chang Je Park
Sejong University, 209 Neungdong-ro, Gwangjin-gu, Seoul 143-747, Republic of Korea
*Corresponding author: saedrawash@sju.ac.kr

1. Introduction

The concept of taking credit for the reduction in reactivity due to fuel burnup is commonly referred to as burnup credit. The reduction in reactivity that occurs with fuel burnup is due to the change in concentration of fissile nuclides and the production of actinide and fission product neutron absorbers [1]. Considering the physics, the axial variation of burnup has been investigated and has shown an impact on the neutron multiplication factor in the burnup credit safety analysis.

Recently, the Nuclear Regulatory Commission (NRC) has issued a guidance on burnup credit for spent nuclear fuel storage casks. The guidance recommends using the loading curve (the loading curve represents the burnup and initial enrichment that correspond to a limiting value of k_{eff}) to confirm the assembly to be loaded in the cask, assemblies with insufficient burnup (underburned) are not acceptable for loading [3].

In some cases, an unauthorized loading of assemblies (misloading) happens due to inaccuracies in reactor burnup records or improper assembly identification.

The axial bounding effect on the reactivity change in the fuel storage cask has been studied in this paper. A previous study was done but with uniform axial considerations, others were done on different cases including the most reactive locations. Here, all possible cases were investigated by increasing the number of possible locations with different patterns.

2. Methods and Results

The misload analysis should consider the effects of placing the underburned assemblies in the most reactive positions within the loaded system (middle of the fuel basket).

Several factors cause an increase in reactivity. However, the increase is dominated by the amount by which the actual assembly burnup is less than the minimum burnup values for loading acceptance and the position of the assembly within the cask [3]. Therefore, a variety of cases are considered including fresh fuel with axial variation of the burnup.

A generic 32 PWR-assembly (GBC-32) cask was used for the analysis with fuel design WE 17x17 fuel assembly as shown in Fig 1. For all assemblies with all cases a 5 years cooling period with assembly-averaged discharge burnup 45GWd/MTU and 4.89% U^{235} enrichment are used throughout this study.

A loading curve shown in Fig 2 has been used for the acceptance loading [4].

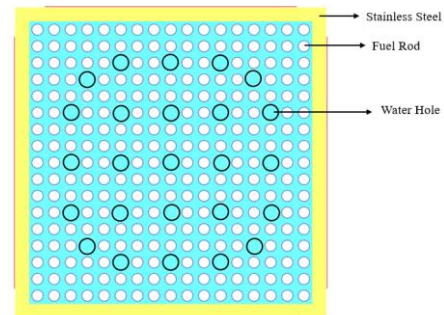


Fig 1. cross-sectional view of an 17x17 Type assembly in KENO VI of the GBC-32 cask.

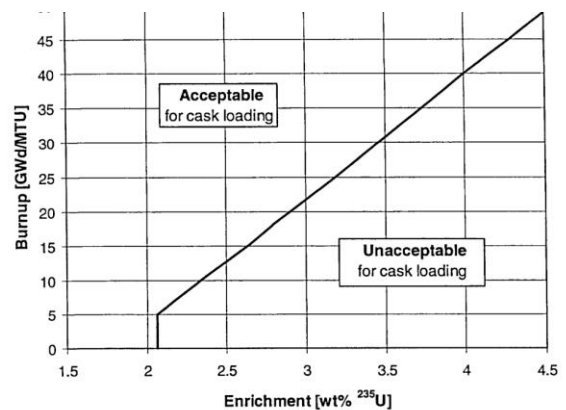


Fig 2. Burnup-credit loading curve depicting initial enrichment and minimum combinations that define the boundary for loading acceptability [3] (assessment of reactivity margins and loading curve).

A uniform axial burnup profile is generally bounding at low burnups but is increasingly non-conservative at higher burnups due to the increasing relative worth of the fuel ends [2]. Since in this study a high burnup value has been used, the bounding axial burnup profiles is considered with 18 segments. **Table 1** shows the bounding axial burnup profiles by burnup group [7].

Considering the probabilities of different values of underburned fuel assembly, a burnup profile has been selected. For example, 60% underburned of 45GWd/MTU should use the profile number 6.

The neutron multiplication factor has been calculated using the well-known KENO-VI three-dimensional Monte Carlo criticality computer code [8]. To ensure proper convergence and reduce statistical uncertainty,

the calculations simulated 1100 generations, with 2000 neutron histories per generation, and skipped the first 100 generation. While the isotopic depletion and decay analysis sequence has been performed using SCALE 6.1/ ORIGIN-Arp [5].

It is also necessary to define the nuclides included in the criticality models. The Actinides and fission products listed in Table 2 Have been used in the calculations bases on their relative reactivity worth.

Table 1. Bounding profiles by burnup group.

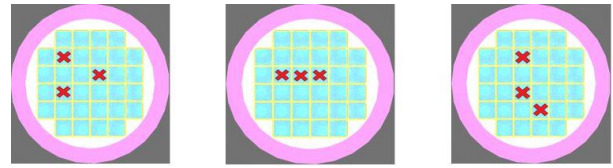
| Burnup groups | Burnup ranges (GWd/MTU) | | | | | | | | | | | |
|------------------|-------------------------|-------|-------|-------|-------|-------|-------|-------|-------|-------|-------|-------|
| | 1 | 2 | 3 | 4 | 5 | 6 | 7 | 8 | 9 | 10 | 11 | 12 |
| Axial height (%) | >46 | 42-46 | 38-42 | 34-38 | 30-34 | 26-30 | 22-26 | 18-22 | 14-18 | 10-14 | 6-10 | <6 |
| 2.78 | 0.573 | 0.674 | 0.660 | 0.585 | 0.652 | 0.619 | 0.630 | 0.668 | 0.649 | 0.633 | 0.662 | 0.574 |
| 8.33 | 0.917 | 0.949 | 0.936 | 0.957 | 0.967 | 0.924 | 0.936 | 1.034 | 1.044 | 0.989 | 0.931 | 0.947 |
| 13.89 | 1.066 | 1.053 | 1.045 | 1.091 | 1.074 | 1.056 | 1.066 | 1.150 | 1.208 | 1.019 | 1.049 | 1.091 |
| 19.44 | 1.106 | 1.085 | 1.080 | 1.121 | 1.103 | 1.097 | 1.103 | 1.094 | 1.215 | 0.857 | 1.059 | 1.105 |
| 25.00 | 1.114 | 1.095 | 1.091 | 1.126 | 1.108 | 1.103 | 1.108 | 1.053 | 1.214 | 0.776 | 1.108 | 1.094 |
| 30.56 | 1.111 | 1.095 | 1.093 | 1.111 | 1.106 | 1.101 | 1.109 | 1.048 | 1.208 | 0.754 | 1.144 | 1.087 |
| 36.11 | 1.106 | 1.093 | 1.092 | 1.094 | 1.102 | 1.103 | 1.112 | 1.064 | 1.197 | 0.785 | 1.168 | 1.086 |
| 41.69 | 1.101 | 1.091 | 1.090 | 1.093 | 1.097 | 1.112 | 1.119 | 1.095 | 1.189 | 1.013 | 1.183 | 1.087 |
| 47.22 | 1.097 | 1.089 | 1.089 | 1.092 | 1.094 | 1.125 | 1.126 | 1.121 | 1.188 | 1.185 | 1.189 | 1.091 |
| 57.80 | 1.093 | 1.088 | 1.088 | 1.091 | 1.094 | 1.136 | 1.132 | 1.135 | 1.192 | 1.253 | 1.190 | 1.096 |
| 58.33 | 1.089 | 1.086 | 1.088 | 1.092 | 1.095 | 1.143 | 1.135 | 1.140 | 1.195 | 1.278 | 1.183 | 1.102 |
| 63.89 | 1.086 | 1.084 | 1.086 | 1.099 | 1.096 | 1.143 | 1.135 | 1.138 | 1.190 | 1.283 | 1.167 | 1.105 |
| 69.44 | 1.081 | 1.081 | 1.084 | 1.096 | 1.095 | 1.136 | 1.129 | 1.130 | 1.156 | 1.276 | 1.135 | 1.105 |
| 75.00 | 1.073 | 1.073 | 1.077 | 1.087 | 1.086 | 1.115 | 1.109 | 1.106 | 1.022 | 1.251 | 1.079 | 1.096 |
| 80.56 | 1.051 | 1.053 | 1.057 | 1.073 | 1.059 | 1.047 | 1.041 | 1.049 | 0.756 | 1.193 | 0.976 | 1.066 |
| 86.11 | 0.993 | 0.987 | 0.996 | 1.003 | 0.971 | 0.882 | 0.871 | 0.933 | 0.614 | 1.075 | 0.806 | 0.986 |
| 91.67 | 0.832 | 0.800 | 0.823 | 0.796 | 0.738 | 0.701 | 0.689 | 0.669 | 0.481 | 0.863 | 0.596 | 0.806 |
| 97.22 | 0.512 | 0.524 | 0.525 | 0.393 | 0.462 | 0.456 | 0.448 | 0.373 | 0.284 | 0.515 | 0.375 | 0.474 |

Table 2. Actinides and fission products for misloading analysis.

| | | | |
|-------------------|-------------------|-------------------|-------------------|
| ²³⁴ U | ²³⁵ U | ²³⁶ U | ²³⁸ U |
| ²³⁷ Np | ²³⁸ Pu | ²³⁹ Pu | ²⁴⁰ Pu |
| ²⁴¹ Pu | ²⁴² Pu | ²⁴¹ Am | ²⁴³ Am |
| ⁹⁵ Mo | ⁹⁹ Tc | ¹⁰¹ Ru | ¹⁰³ Rh |
| ¹⁰⁹ Ag | ¹³³ Cs | ¹⁴³ Nd | ¹⁴⁵ Nd |
| ¹⁴⁷ Sm | ¹⁴⁹ Sm | ¹⁵⁰ Sm | ¹⁵¹ Sm |
| ¹⁵³ Eu | ¹⁵⁵ Gd | ¹⁶ O | ¹⁵² Sm |

The investigation is done on the misloading of fuel assemblies in the inner 16 locations of the cask since these are the most reactive locations which has the greater effect on the reactivity change. In addition, it will take lots of calculations and time for all the 32 locations. The underburned fuel values range from 100% to 0% of the minimum value required by the loading curve with 10% decrement. Multiple underburned fuel assemblies have been considered in the study from 1 to 16 misloading's. A 3 misloading cases are shown in Fig 3.

Fig 3. Three Cases for 3 misloading (underburned) Fuel Assemblies.



Using all possibilities of the 16 locations with multiple ranges of underburned fuel assemblies, the total cases are 11 (90% to 0% including fully burned 100%) multiply by possibilities of locations which are 511 cases for 1 to 16 underburned assembly. In this paper the k_{eff} for 9 misloading fuel assemblies will be shown in Table 3 since it will be difficult to show all the cases.

Table 3. k_{eff} changes with different values of underburned fuel assembly for 9 misloading's of limiting value 45GWd/MTU and 4.89% U235.

| Burnup % | k-eff | dK |
|----------|---------|-----------|
| 100 | 0.89537 | ± 0.00063 |
| 90 | 0.90338 | ± 0.00064 |
| 80 | 0.92050 | ± 0.00056 |
| 70 | 0.93342 | ± 0.00064 |
| 60 | 0.95064 | ± 0.00059 |
| 50 | 0.96548 | ± 0.00058 |
| 40 | 0.98165 | ± 0.00064 |
| 30 | 1.01312 | ± 0.00057 |
| 20 | 1.02103 | ± 0.00061 |
| 10 | 1.04097 | ± 0.00064 |
| 0 | 1.06994 | ± 0.00076 |

The target k_{eff} for this research was 0.95 as safety margin. From Table 3 it is clearly shown that for 9 misloading assemblies it is acceptable to load 9 underburned fuel assemblies in the spent fuel storage cask up to 60% underburned of the acceptable burnup value.

As a result of the calculations for all multiple underburned assemblies' possibilities, the 0% is unacceptable since k_{eff} is higher than 0.95 of the acceptable safety margins. While even for large number of underburned fuel assemblies, the loading is acceptable up to 60% underburned for all multiple cases from 1 to 16 fuel assemblies.

As the change of reactivity is due to the change in the concentrations of the nuclides in the fuel rod. It is necessary to show this change. Tables 4 and 5 show all nuclides used in the calculation for 60% and 100% underburned of 45GWd/MTU and 4.89% U^{235} for three segments of the fuel rod, the most end segments and the middle one. The isotopic concentrations have been calculated using ORIGEN-ARP a SCALE isotopic and decay analysis [6].

As been noticed from Tables 4 and 5, the nuclides concentrations are clearly higher in the 60% underburned than the 100% case, which gives a higher reactivity worth. In the meanwhile, the lower and upper ends having higher concentrations rather than the middle due to the neutron leakage.

Due to many results, few cases result for k_{eff} are shown in this study. Tables 6 and 7 show 10 k_{eff} result for 3 misloading's. A 35 cases have been calculated with different fuel assembly locations.

Table 4. Nuclides concentration variations with 18 segments axially for 60% of 45GWd/MTU and 4.89% U^{235} .

| Nuclides | Atoms/b-cm Upper End segment 16713 MWD/MTU | Atoms/b-cm middle segment 30024 MWD/MTU | Atoms/b-cm Lower End segment 12312 MWD/MTU |
|----------|--|---|--|
| u-234 | 8.856E-06 | 7.500E-06 | 9.345E-06 |
| u-235 | 7.832E-04 | 5.315E-04 | 8.818E-04 |
| u-236 | 8.506E-05 | 1.277E-04 | 6.728E-05 |
| u-238 | 2.300E-02 | 2.279E-02 | 2.306E-02 |
| np-237 | 4.368E-06 | 1.004E-05 | 2.795E-06 |
| pu-238 | 5.008E-07 | 2.205E-06 | 2.300E-07 |
| pu-239 | 1.148E-04 | 1.466E-04 | 9.589E-05 |
| pu-240 | 2.006E-05 | 4.092E-05 | 1.314E-05 |
| pu-241 | 7.964E-06 | 2.002E-05 | 4.368E-06 |
| pu-242 | 1.071E-06 | 5.502E-06 | 4.117E-07 |
| am-241 | 2.263E-06 | 5.853E-06 | 1.227E-06 |
| am-243 | 8.819E-08 | 8.754E-07 | 2.388E-08 |
| mo-95 | 2.659E-05 | 4.551E-05 | 1.990E-05 |
| tc-99 | 2.620E-05 | 4.474E-05 | 1.963E-05 |
| ru-101 | 2.296E-05 | 4.097E-05 | 1.694E-05 |
| rh-103 | 1.474E-05 | 2.541E-05 | 1.092E-05 |
| ag-109 | 1.032E-06 | 2.620E-06 | 6.296E-07 |
| cs-133 | 2.781E-05 | 4.760E-05 | 2.078E-05 |
| nd-143 | 2.241E-05 | 3.569E-05 | 1.716E-05 |
| nd-145 | 1.579E-05 | 2.657E-05 | 1.189E-05 |
| sm-147 | 5.682E-06 | 8.368E-06 | 4.475E-06 |
| sm-149 | 2.208E-07 | 2.416E-07 | 2.083E-07 |
| sm-150 | 5.397E-06 | 1.055E-05 | 3.791E-06 |
| sm-151 | 5.767E-07 | 7.088E-07 | 5.170E-07 |
| eu-151 | 2.319E-08 | 2.847E-08 | 2.077E-08 |
| sm-152 | 2.458E-06 | 4.375E-06 | 1.762E-06 |
| eu-153 | 1.415E-06 | 3.351E-06 | 9.087E-07 |
| gd-155 | 3.047E-08 | 7.398E-08 | 2.131E-08 |
| O-16 | 0.0489 | 0.0489 | 0.0489 |

Table 5. Nuclides concentration variations with 18 segments axially for 100% of 45GWd/MTU and 4.89% U^{235} .

| Nuclides | Atoms/b-cm End segment 3033 MWD/MTU | Atoms/b-cm middle segment 49185 MWD/MTU | Atoms/b-cm End segment 23580 MWD/MTU |
|----------|---|--|--|
| u-234 | 7.471E-06 | 5.869E-06 | 8.133E-06 |
| u-235 | 5.265E-04 | 2.744E-04 | 6.451E-04 |
| u-236 | 1.285E-04 | 1.637E-04 | 1.090E-04 |
| u-238 | 2.278E-02 | 2.244E-02 | 2.289E-02 |
| np-237 | 1.018E-05 | 1.876E-05 | 7.172E-06 |
| pu-238 | 2.262E-06 | 7.254E-06 | 1.201E-06 |
| pu-239 | 1.470E-04 | 1.572E-04 | 1.349E-04 |
| pu-240 | 4.138E-05 | 6.559E-05 | 3.100E-05 |
| pu-241 | 2.028E-05 | 3.326E-05 | 1.423E-05 |
| pu-242 | 5.646E-06 | 1.764E-05 | 2.895E-06 |
| am-241 | 5.933E-06 | 9.957E-06 | 4.109E-06 |
| am-243 | 9.084E-07 | 4.621E-06 | 3.525E-07 |
| mo-95 | 4.592E-05 | 6.945E-05 | 3.660E-05 |
| tc-99 | 4.514E-05 | 6.812E-05 | 3.601E-05 |
| ru-101 | 4.138E-05 | 6.628E-05 | 3.230E-05 |
| rh-103 | 2.564E-05 | 3.775E-05 | 2.044E-05 |
| ag-109 | 2.661E-06 | 5.562E-06 | 1.791E-06 |
| cs-133 | 4.803E-05 | 7.227E-05 | 3.829E-05 |
| nd-143 | 3.595E-05 | 4.807E-05 | 2.974E-05 |
| nd-145 | 2.680E-05 | 3.958E-05 | 2.154E-05 |
| sm-147 | 8.415E-06 | 1.029E-05 | 7.233E-06 |
| sm-149 | 2.419E-07 | 2.381E-07 | 2.342E-07 |
| sm-150 | 1.067E-05 | 1.864E-05 | 8.020E-06 |
| sm-151 | 7.116E-07 | 8.725E-07 | 6.478E-07 |
| eu-151 | 2.858E-08 | 3.492E-08 | 2.604E-08 |
| sm-152 | 4.416E-06 | 6.751E-06 | 3.486E-06 |
| eu-153 | 3.400E-06 | 6.670E-06 | 2.355E-06 |
| gd-155 | 7.524E-08 | 1.684E-07 | 5.009E-08 |
| O-16 | 4.89E-02 | 4.89E-02 | 4.89E-02 |

Table 6. k_{eff} for 10 cases out of 35 cases for 3 misloading fuel assemblies for 0% underburned (fresh fuel). 45GWd/MTU and 4.89% U^{235} .

| Cases | k_{eff} |
|---------|-----------|
| Case 1 | 1.04033 |
| Case 2 | 0.98893 |
| Case 3 | 1.04993 |
| Case 4 | 0.98163 |
| Case 5 | 0.98006 |
| Case 6 | 0.99069 |
| Case 7 | 1.04834 |
| Case 8 | 0.9723 |
| Case 9 | 0.96732 |
| Case 10 | 0.98919 |

Table 7. k_{eff} for 10 cases out of 35 cases for 3 misloading assemblies for 90% underburned. 45GWd/MTU and 4.89% U^{235} .

| Cases | k_{eff} |
|---------|-----------|
| Case 1 | 0.89663 |
| Case 2 | 0.89712 |
| Case 3 | 0.89684 |
| Case 4 | 0.89648 |
| Case 5 | 0.89798 |
| Case 6 | 0.90014 |
| Case 7 | 0.89589 |
| Case 8 | 0.89617 |
| Case 9 | 0.89982 |
| Case 10 | 0.89725 |

From Table 6 Misloading is not allowed for fresh fuel case since all values of k_{eff} are higher than 0.95. while in figure 7 for the 90% underburned, all cases are acceptable.

In addition to addressing the axial bounding burnup calculations. One case (9 misloading's case) of uniform burnup profile has been studied as comparison to the axial variation of the burnup as shown in Table 8 below.

Table 8. A comparison between uniform and axial burnup profiles for burnup credit calculations for 9 misloading's case study.

| Burnup | K_{eff} at 90% underburned | K_{eff} at 0% underburned |
|---------|------------------------------|-----------------------------|
| Uniform | 0.87475 | 1.07265 |
| Axial | 0.90338 | 1.06994 |

As shown in Table 8, there is a clear impact of addressing the axial variation in the calculation for the burnup credit safety analysis. The 0.02863 difference between the uniform and bounding burnup profiles for the 90% underburned case, which comes from the physical behavior of the neutron flux where is more neutron leakage in the fuel ends leaving more nuclides in the spent fuel without burning.

3. Conclusions

The axial burnup effect on multiple cases of misloading fuel assemblies has been studied. It is concluded that the axial variation has an impact on the neutron multiplication factor which can not be ignored in analyzing the criticality safety report for the spent fuel storage cask. One case shows that there is 0.02863 difference in k_{eff} from the uniform burnup profile.

This study has shown also how the reactivity changes by amount of the fuel is underburned and the location being loaded. It has been noticed that the margin for loading an underburned fuel is up to 60% of the acceptable burnup value related to the loading curve with a 0.95 k_{eff} as a safety margin.

In the future, more precise analysis will be carried out, such as the cooling periods and different initial enrichments.

REFERENCES

[1] J.C. Wagner, Criticality Analysis of Assembly Misload in a PWR Burnup Credit Cask, NUREG/CR-6955 (ORNL/TM-2004/52), U.S. Nuclear Regulatory Commission, Oak Ridge National Laboratory, January 2008.
 [2] J.C. Wagner, M.D. DeHart, and C.V. Parks, recommendations for Addressing Axial Burnup in PWR Burnup Credit,

NUREG/CR-6801 (ORNL/TM-2001/273), U.S. Nuclear Regulatory Commission, Oak Ridge National Laboratory, March 2003.

[3] U.S Nuclear Regulatory Commission, Spent Fuel Project Office Interim Staff Guidance-8, Rev. 3-Burnup Credit in the Criticality Safety Analyses of PWR Spent Fuel in Transport and Storage Casks, U.S. Nuclear Regulatory Commission, September 27, 2002.

[4] J.C Wagner and C.E. Sanders, Assessment of Reactivity Margins and Loading Curves for PWR Burnup-Credit Cask Designs, NUREG/CR-6800 (ORNL/TM-2002/6), U.S. Nuclear Regulatory Commission, Oak Ridge National Laboratory, March 2003.

[5] SCALE: A Modular Code System for Performing Standardized Computer Analyses for Licensing Evaluation, NUREG/CR-0200, Rev.6 (ORNL/NUREG/CSD-2/R6), Vols. I, II, and III, May 2000. Available from Radiation Safety Information Computational Center at Oak Ridge National Laboratory as CCC-545.

[6] S.M. Browman and L.C. Leal, "ORIGEN-ARP. Automatic Rapid Process for Spent Fuel Depletion, Decay, and Source Term Analysis," Vol I, Sect. D1 of SCALE: A Modular Code System for Performing Standardized Computer Analyses for Licensing Evaluation, NUREG/CR-0200, Rev 6 (ORNL/NUREG/CSD-2/R6), Vols. I, II, and III, May 2000. Available from Radiation Safety Information Computational Center at Oak Ridge National Laboratory as CCC-545.

[7] T. A. Parish and C. H. Chen, Bounding Axial Profile Analysis for the Topical Report Database, Nuclear Engineering Dept, Texas A&M University, May 1997.

[8] L.M. Petrie and N.F. Landers, "KENO VI: An Improved Monte Carlo Criticality Program with Supergrouping," Vol. II of SCALE: A Modular Code System for Performing Standardized Computer Analyses for Licensing Evaluation, NUREG/CR-0200, Rev 6 (ORNL/NUREG/CSD-2/R6), Vols. I, II, and III, May 2000. Available from Radiation Safety Information Computational Center at Oak Ridge National Laboratory as CCC-545.